JOURNAL OF VIROLOGY, May 2002, p. 4401–4411 Vol. 76, No. 9
0022-538X/02/$04.00+0 DOI: 10.1128/JVI.76.9.4401–4411.2002

Role of Recycling Endosomes and Lysosomes in Dynein-Dependent Entry of Canine Parvovirus

Sanna Suikkanen, Katja Sääjärvi, Jonna Hirsimäki, Outi Välilehto, Hilkka Reunanen, Maija Vihinen-Ranta, and Matti Vuento*

Department of Biological and Environmental Science, University of Jyväskylä, SF-40500 Jyväskylä, Finland

Received 3 October 2001/Accepted 29 January 2002

Canine parvovirus (CPV) is a nonenveloped virus with a 5-kb single-stranded DNA genome. Lysosomotropic agents and low temperature are known to prevent CPV infection, indicating that the virus enters its host cells by endocytosis and requires an acidic intracellular compartment for penetration into the cytoplasm. After escape from the endocytotic vesicles, CPV is transported to the nucleus for replication. In the present study the intracellular entry pathway of the canine parvovirus in NLFK (Nordisk Laboratory feline kidney) cells was studied. After clustering in clathrin-coated pits and being taken up in coated vesicles, CPV colocalized with coendocytosed transferrin in endosomes resembling recycling endosomes. Later, CPV was found to enter, via late endosomes, a perinuclear vesicular compartment, where it colocalized with lysosomal markers. There was no indication of CPV entry into the trans-Golgi or the endoplasmic reticulum. Similar results were obtained both with full and with empty capsids. The data thus suggest that CPV or its DNA was released from the lysosomal compartment to the cytoplasm to be then transported to the nucleus. Electron microscopy analysis revealed endosomal vesicles containing CPV to be associated with microtubules. In the presence of nocodazole, a microtubule-disrupting drug, CPV entry was blocked and the virus was found in peripheral vesicles. Thus, some step(s) of the entry process were dependent on microtubules. Microinjection of antibodies to dynein caused CPV to remain in pericellular vesicles. This suggests an important role for the motor protein dynein in transporting vesicles containing CPV along the microtubule network.

The parvovirus family consists of a large number of viruses that infect hosts from insects to humans. The canine parvovirus (CPV), a member of the autonomous *Parvovirus* genus (38), is a small nonenveloped virus which has a single-stranded DNA genome and which replicates in the nucleus of actively dividing cells (10).

It has been established that nonenveloped viruses gain entry to their host cells by one of several mechanisms. Adenoviruses bind to a cell receptor via the fiber protein. For internalization, a second protein-protein recognition event is needed in which the penton base interacts with integrin. The virion is internalized by endocytosis. The viral capsid proteins are sequentially removed in endosomes. Finally, an acid-activated membranelytic protein disrupts the endosomal membranes, allowing the capsids to be released from the late endosomal compartment into the cytoplasm for nuclear transport (5, 13, 32). Some picornaviruses undergo receptor-mediated conformational changes and form altered particles in which the hydrophobic amino terminus of virus protein 1 (VP1) is exposed on the virion surface (6). The amino terminus of VP1 is believed to form a pore in the cell membrane through which the RNA is released from the capsid into the cytoplasm (12, 29, 41). Members of the *Reoviridae* take advantage of lysosomal proteases and nucleases in their uncoating process, which takes place in lysosomes. The virus undergoes several disassembly steps during endocytosis. Proteolysis in late endosomes produces infectious subviral particles, which penetrate through the lysosomal membranes and enter the cytoplasm as core particles to initiate RNA synthesis (8, 21, 42). Simian virus 40, a nonenveloped DNA virus of the *Polyomaviridae* family, enters cells through the caveolae (1, 28, 33) and accumulates in the smooth endoplasmic reticulum (ER) via organelles with a nonacidic pH. Virions are transported to the perinuclear area in tubular membrane extensions along microtubules (28).

Details of the intracellular pathway used by parvoviruses are not fully understood. Recent data on feline and mink cell lines have shown that CPV uses the transferrin receptor to attach and infect cells (25). Adeno-associated viruses (AAVs), members of the *Dependovirus* genus of parvoviruses, are known to bind heparan sulfate proteoglygans (AAV serotype 2 [36]) or sialic acid (AAV serotypes 4 and 5 [17]) on the surface of the host cell. The virus and its receptor enter host cells via dynamin-dependent and clathrin-mediated endocytosis (2, 3, 9, 10, 26). Both AAV and CPV infections could be blocked by lysosomotropic agents, suggesting that low pH is essential for the entry of these viruses (2, 3, 7, 26, 44). The infectious entry of CPV could also be blocked by the disruption of microtubules and by low temperature, suggesting the involvement of microtubule-dependent vesicle trafficking (44). CPV particles colocalized with transferrin in perinuclear endosomes of Mv1Lu cells transfected with human transferrin receptor (25), suggesting the endocytic uptake via the pericentriolar recycling compartment.

There is some evidence indicating that the release of CPV from endocytotic vesicles is extremely slow. A selective inhibitor of the vacuolar H^+-ATPase, bafilomycin A1, has been

* Corresponding author. Mailing address: Department of Biological and Environmental Science, University of Jyväskylä, Survontie 9, SF-40500 Jyväskylä, Finland. Phone: 358-14-260-2282. Fax: 358-14-260-2271. E-mail: vuento@dodo.jyu.fi.

used to determine the requirement of acidic endosomal compartments for viral entry (4, 29). When applied at 90 min postinfection (p.i.) the drug inhibited infection by CPV (26). Antibodies to CPV capsid proteins microinjected into the cytoplasm, even as late as 6 h p.i., prevented infection, suggesting that viral capsids remain in endocytic vesicles for several hours after uptake (45). These results suggest that capsids entering the cell may be transported from recycling endosomes to another vesicular compartment before penetration to the cytoplasm (26, 44). In contrast to the slow penetration of CPV from endosomal vesicles, it has been suggested that AAV penetrates from early endosomes into the cytoplasm as early as 30 min p.i. and reaches the nucleus within 2 h p.i. (2). Recently, AAV particles were reported to reach the late endosomal compartment before release and to be degraded in a significant proportion by the proteasome (7).

Given the known complexity of the endosomal compartments involved in vesicle trafficking, our purpose here was to clarify in greater depth the intracellular entry route used by CPV. In the present study the infectious entry of CPV was investigated by using immunoelectron microscopy, laser scanning confocal microscopy, and fluorescence in situ hybridization to follow the detailed pathway of CPV proteins and DNA in infected cells.

MATERIALS AND METHODS

Cells and viruses. NLFK cells (a gift from Colin Parrish, Cornell University, Ithaca, N.Y.) were grown and maintained in Dulbecco modified Eagle medium (DMEM) supplemented with 10% fetal calf serum (Gibco, Paisley, United Kingdom). Canine parvovirus type 2 (CPV-d), derived from a plasmid clone of virus (27), was grown in NLFK cells in 175-cm^2 cell culture flasks (Nunc, Roskilde, Denmark) for 5 to 7 days and then stored at −20°C. Then, 300 ml of culture medium from infected cells was clarified by centrifugation and concentrated by ultrafiltration (30-kDa filter; Millipore Corp., Bedford, Mass.). The CPV was pelleted by ultracentrifugation at 173,000 × *g* for 1 h and resuspended in 0.9 ml of phosphate-buffered saline (pH 7.4) (PBS). The suspension was sonicated at low power and extracted with chloroform. Full (heavy fraction, H-CPV) and empty (light fraction, L-CPV) capsids were purified from the aqueous phase by isopycnic centrifugation in a 45% cesium chloride gradient. Two opalescent bands, one representing empty capsids and the other full capsids, were observed and collected separately with a syringe. The capsids were pelleted again by ultracentrifugation at 245,000 × *g* for 2 h and resuspended in 200 μl of PBS. Empty capsids were tested (see below) and were not infective.

Immunofluorescence microscopy. For the immunofluorescence studies, cells grown to 80% confluency on coverslips (diameter, 13 mm) were inoculated with full or empty capsids for 15 min at 37°C. At set intervals p.i. the coverslips were dipped in PBS and fixed with 4% paraformaldehyde in PBS. After permeabilization with 1% bovine serum albumin, 1% Triton X-100, and 0.01% sodium azide in PBS for 15 min, the coverslips were incubated for 45 min at room temperature with primary antibodies diluted in permeabilization buffer and then rinsed several times. The coverslips were incubated with the appropriate labeled secondary antibody for 45 min. Before they were embedded with Mowiol and with antifading agent DABCO (30 mg/ml; Sigma, St. Louis, Mo.), the coverslips were rinsed several times. The samples were examined with a laser scanning fluorescence microscope (LSM 510; Zeiss Axiovert 100 M) by using the excitation and emission settings appropriate for the dye used.

Determination of infectivity. Infectivity was determined by calculating the ratio of cells with fluorescent nuclei to the total number of cells ($n = 300$) at 24 h p.i. by immunofluorescence with polyclonal antibody (Cornell no. 2 [see below]) to CPV.

Antibodies. Rabbit antibody to CPV capsid, mouse monoclonal antibody (hybridoma culture medium, MAb 8 [35]) to CPV capsid and mouse monoclonal antibody to nonstructural protein 1 (NS1) were gifts from Colin Parrish (Cornell University, Ithaca, N.Y.) Mouse monoclonal antibody against TGN-38 was from Sigma. Antibody against lysosomal glycoprotein LAMP-2 was from Developmental Studies Hybridoma Bank, The University of Iowa, Iowa City. Polyclonal rabbit antiserum to β-COP was a generous gift from Albrecht Gruhler (R. W. Johnson Pharmaceutical Research Institute, San Diego, Calif.). Rabbit antiserum to caveolin and affinity-purified rabbit antibody against cation-independent mannose-6-phosphate receptor (MPR) were kindly provided by Varpu Marjomäki (University of Jyväskylä, Jyväskylä, Finland) (19). Antibody to protein disulfide isomerase (PDI; clone 1D3) a marker for ER, was obtained from Stephen Fuller (Wellcome Trust Centre for Human Genetics, University of Oxford, Oxford, United Kingdom) (16). For signal enhancement in in situ hybridization, we used biotinylated goat anti-streptavidin antibody (Molecular Probes, Eugene, Oreg.). Anti-dynein and anti-kinesin antibodies (Chemicon, Temecula, Calif.) were used in the microinjection experiments after dialysis against 10 mM Tris-HCl–120 mM KCl (pH 7.9). Monoclonal anti-tubulin antibody was from Amersham, Buckinghamshire, United Kingdom. Fluorescein-conjugated anti-mouse antibody, rhodamine-conjugated anti-rabbit antibody, and TRITC (tetramethyl rhodamine isocyanate)-conjugated goat anti-rabbit antibody were from Cappel/ICN Pharmaceuticals, Inc. In the double-labeling studies, Alexa-546-conjugated anti-mouse antibody and Alexa-488-conjugated anti-rabbit antibody purchased from Molecular Probes were used as secondary antibodies. Streptavidin-Alexa 488 and biotinylated goat anti-streptavidin antibody, as well as Alexa 488-labeled anti-goat immunoglobulin antibody, used in the fluorescence in situ hybridization, were from Molecular Probes.

Reagents. Nocodazole (Sigma) was used for the depolymerization of microtubules. Gold-conjugated protein A (10 nm) was from G. Posthuma, University of Utrecht, Utrecht, The Netherlands. Human holo-transferrin (Sigma) was used as a marker for recycling endosomes.

Microinjection. For the microinjection experiments, cells were grown to 80% confluency on Microgrid coverslips (175-μm grid size; Eppendorf, Hamburg, Germany). Anti-dynein and anti-kinesin antibodies were dialyzed against 10 mM Tris-HCl–120 mM KCl (pH 7.9). Cells were microinjected with 0.1 to 0.5 pl of antibody at 3 to 5 mg/ml by using an Eppendorf 5246 microinjector and an Eppendorf 5171 micromanipulator. Capillaries were pulled with a Flaming/Brown Micropipette puller. After 20 min of incubation, the cells were inoculated with CPV for 15 min, at 37°C. After 2 h from the time of inoculation, the cells were fixed with methanol. CPV, microinjected antibody, and microinjected control antibody were detected by immunofluorescence techniques.

Immunoelectron microscopy. A JEOL JEM-1200EX transmission electron microscope operated at ~60 kV was used in the preembedding or cryosectioning electron microscopy.

Preembedding electron microscopy. Cells were grown on 35-mm plastic culture dishes to 80% confluency. After they were rinsed with ice-cold 0.1 M phosphate buffer (pH 7.4), the cells were treated with CPV in DMEM for 1 h on ice. After four washes with ice-cold 0.1 M phosphate buffer, polyclonal rabbit antiserum to CPV diluted in 0.1 M phosphate buffer was applied for 1 h at 0°C, followed by protein-A gold conjugate for 45 min at 0°C. After three washes, the cells were either fixed immediately with 2.5% glutaraldehyde in 0.1 M phosphate buffer for 1 h at 4°C or warmed up in DMEM to 37°C for various periods (0.5 to 3 h) of time. After three rinses in 0.1 M phosphate buffer (pH 7.4), the cell cultures were postfixed in 1% osmium tetroxide in 0.1 M phosphate buffer for 1 h at 4°C and dehydrated in ethanol, stained with uranyl acetate, and embedded in LX-112. Thin sections were cut and poststained with lead citrate and uranyl acetate.

Cryosectioning. The cells were inoculated with CPV for 15 min at 37°C and incubated in DMEM for 1 h or 3 h, the dishes were washed two times with PBS, and the cells were fixed with 4% paraformaldehyde, 0.1% glutaraldehyde, 0.01 sodium azide, and 7.5% sucrose in PBS for 1 h at room temperature. After fixation, the cells were washed with PBS and scraped off with a rubber policeman, sedimented, gently resuspended in 10% warm gelatin in PBS, and further processed for cryosections and immunogold labeling as described previously (39, 40). The sections were labeled with mouse monoclonal antibody to CPV capsid, followed by the addition of rabbit anti-mouse antibody and gold-conjugated protein A. The sections were incubated for 45 min at room temperature and washed with PBS after each labeling step.

Fluorescence in situ hybridization. Plasmid p265 containing the total genomic sequence of CPV (a gift from Colin Parrish) was labeled with Biotin Nick-Translation Mix (Boehringer Mannheim, Mannheim, Germany). The size of the labeled probe was analyzed with electrophoresis and found to be 200 to 500 nucleotides long. The probe was separated from the labeling mixture by precipitation with ethanol. NLFK cells were grown on coverslips (diameter, 13 mm) to 80% confluency and inoculated with purified CPV for 15 min at 37°C, after which they were incubated in DMEM for 0 to 24 h. Coverslips were dipped in PBS and fixed with methanol. After three washes with PBS, the capsid proteins were labeled with polyclonal antibody and TRITC-conjugated anti-rabbit antibody. The samples were then postfixed with 1% paraformaldehyde. Cells were washed with PBS and then dehydrated and rehydrated with alcohol series (70, 90, 100,

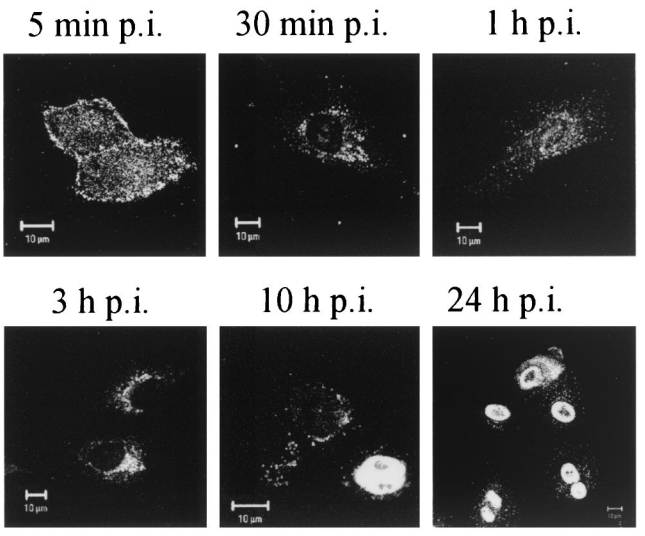

FIG. 1. Localization of CPV capsid proteins in NLFK cells during the infection cycle. Confocal immunofluorescence images of infected cells, fixed at time points p.i., are shown in the figure. CPV was detected with polyclonal antibody to CPV capsid and with TRITC-labeled goat anti-rabbit antibody as a secondary antibody. Bar, 10 nm.

90, and 70%) for 30 s each. Hybridization was carried out in buffer containing 60% deionized formamide, 1.5 M NaCl, 0.15 M sodium citrate, 10 mM EDTA, 25 mM NaH_2PO_4, 5% dextran sulfate, 250 ng of herring sperm DNA/μl, and 30 ng of probe/μl. The probe was denatured for 5 min at 80°C and hybridized in 50% deionized formamide, 0.3 M NaCl, and 0.03 M sodium citrate in a humid chamber overnight at 37°C. Coverslips were washed two times with 1.5 M NaCl and 0.15 M sodium citrate in 50% deionized formamide and two times with PBS. Samples were blocked with 3% bovine serum albumin-PBS for 10 min. The following incubations were carried out in a humid chamber for 1 h at room temperature. The biotinylated probe was first complexed with two layers of streptavidin-Alexa 488. These were then conjugated with biotinylated goat anti-streptavidin antibody. Finally, anti-streptavidin antibody was labeled with anti-goat Alexa 488. Samples were mounted in Mowiol with DABCO (30 mg/ml) and examined with the LSM.

RESULTS

The general course of infection. The results from the immunofluorescence microscopy illustrate the general course of infection of NLFK cells by CPV (Fig. 1). At 5 min p.i., CPV was found on the cell surface, as well as in endosomal vesicles in the cellular periphery. At 30 min p.i., CPV was no longer found on the cell surface but in intracellular vesicles that, with time (1 to 3 h p.i.), acquired an increasingly perinuclear, usually polar, location. This location of CPV in perinuclear vesicles remained essentially unchanged up to 10 h p.i. However, at 10 h p.i. CPV antigens were also found in the nucleus. While this could mean that CPV or its capsid proteins had substantially entered the nucleus, the result could also reflect the import of freshly synthesized capsid proteins. When antibody to NS1 protein was used instead of antibody to capsid protein, fluorescent nuclei were observed as early as 8 h p.i. (not shown). At 24 h p.i. the nuclei were strongly fluorescent, indicating the onset of synthesis and nuclear transport of viral proteins (Fig. 1). It is this general frame of events that we attempt to dissect into defined steps below.

Binding to cell surface and uptake of CPV to coated vesicles. Given the superiority of resolution of electron microscopy to that of fluorescence microscopy, it was of interest to study the early events of CPV entry by using immunoelectron microscopy. At 0 min p.i., gold particles tracing antibody bound to CPV were first found on the cell surface in pits with an electron-dense coating resembling clathrin (Fig. 2A). At 5 min p.i., coated vesicles containing gold particles were detected near the plasma membrane (Fig. 2B). At this time, gold particles were also detected in early endosome-like structures (Fig. 2C). While these results were in agreement with the idea that CPV enters via clathrin-coated vesicles, it was of interest to study whether this type of entry was exclusively used. During the first 30 min of infection CPV was not detected in small noncoated vesicles in immunoelectron microscopy (Fig. 3A). CPV did not colocalize at all with caveolae in the double-labeling studies with the LSM (Fig. 3B).

Dependency of CPV entry on microtubules and dynein. In LSM experiments, CPV was found to be transported to a perinuclear area during the first 3 h of infection (Fig. 1). At 30 min to 1 h p.i. we found, by immunoelectron microscopy, CPV immunoreactivity in vesicles located along the microtubules (Fig. 4). The vesicles seemed to be connected to microtubules by electron-dense material (Fig. 4, arrow). Disruption of the microtubule network with nocodazole caused the viral antigens to remain in the cellular periphery 12 h after uptake, while in

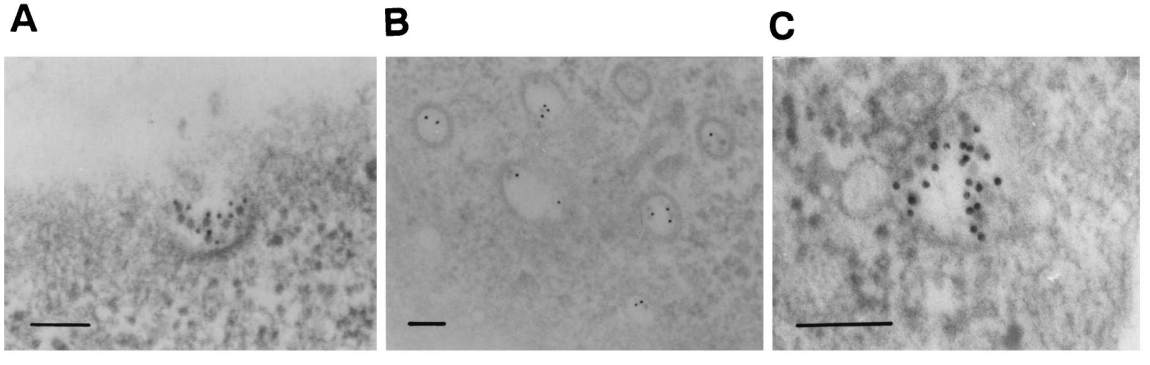

FIG. 2. Immunoelectron microscopy analysis of CPV binding and uptake into the NLFK cells. CPV was detected with polyclonal anti-capsid antibody, which was visualized with protein A-gold conjugate (10 nm) by using the preembedding technique. Cells were fixed after adsorption at 0 min p.i. (A), 5 min p.i. (B), and 5 min p.i. (C). Bar, 100 nm.

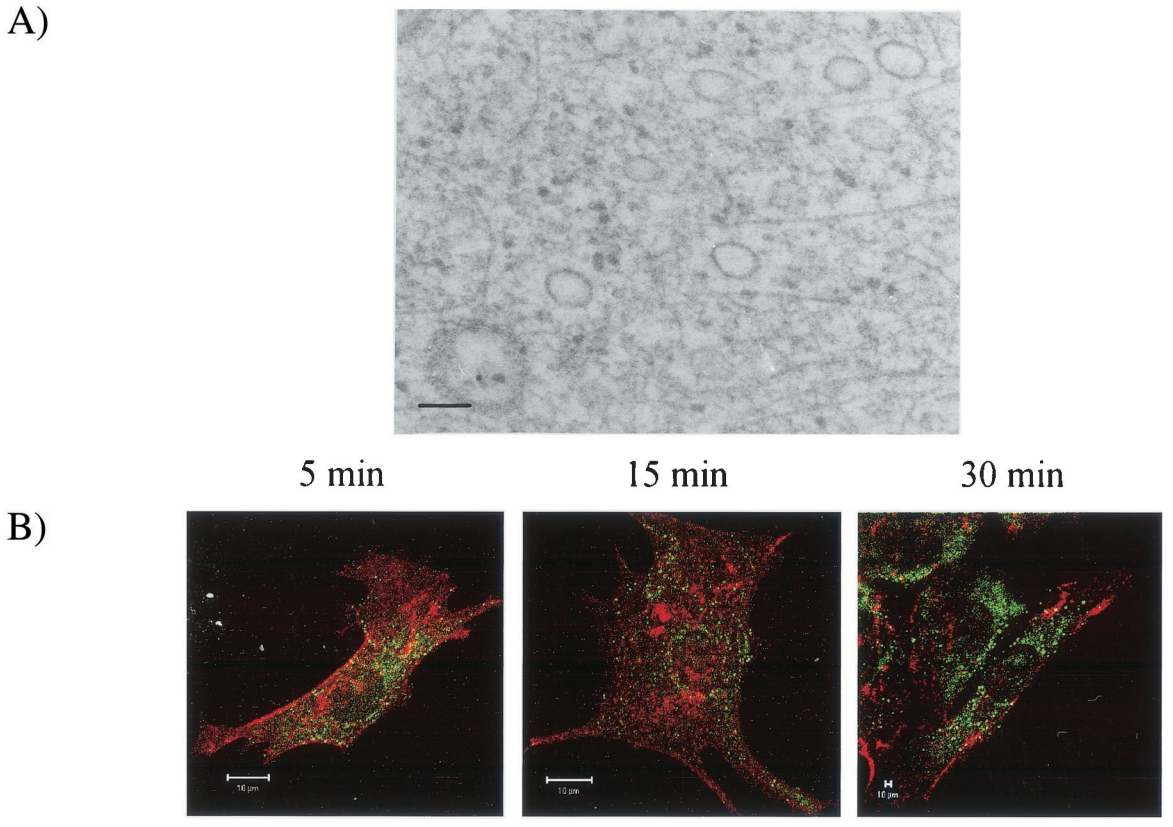

FIG. 3. Localization of CPV capsid proteins and caveolae during early steps of infection. (A) Immunoelectron microscopy (preembedding) at 5 min p.i. Bar, 100 nm. (B) Confocal images. Color: red, caveolae; green, CPV; yellow, colocalization. Bar, 10 μm.

control cells viral immunoreactivity was detected in the nucleus (Fig. 5). These results illustrated the importance of microtubules for CPV entry. In light of the known role of dynein and kinesin in transporting the vesicular cargo along microtubules, we sought to clarify whether these motor proteins were involved in transporting vesicles containing CPV. At 0 to 1 h p.i., we microinjected anti-kinesin and anti-dynein antibodies to the cytoplasm of the cells before inoculation with CPV. Successful microinjection was verified by detecting the injected antibody (Fig. 6A and C). In cells microinjected with anti-dynein antibody, vesicles containing CPV were found in the cellular periphery, while in control cells CPV was detected in the perinuclear area (Fig. 6B). Cytoplasmic microinjection of anti-kinesin antibody did not cause notable effects (Fig. 6C). The results suggest a role for dynein in the transport of endocytic vesicles containing CPV.

Characteristics of the perinuclear vesicular compartment containing CPV. At 1 h after inoculation, CPV-immunoreactivity was found in vesicles having a polar, perinuclear location (Fig. 1, 3 and 10 h p.i.). To characterize these vesicles, infected cells were studied with immunoelectron microscopy. In addition, several organelle markers were tested for colocalization

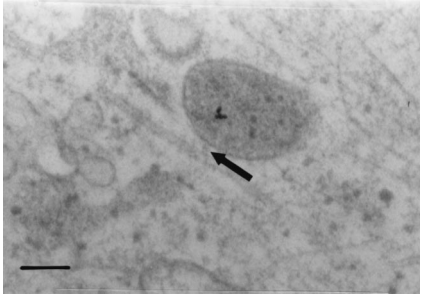

FIG. 4. Association of CPV-containing vesicle with microtubule. Immunoelectron microscopy (preembedding) analysis of CPV at 1 h p.i. was done. For technical details, see the legend to Fig. 1.

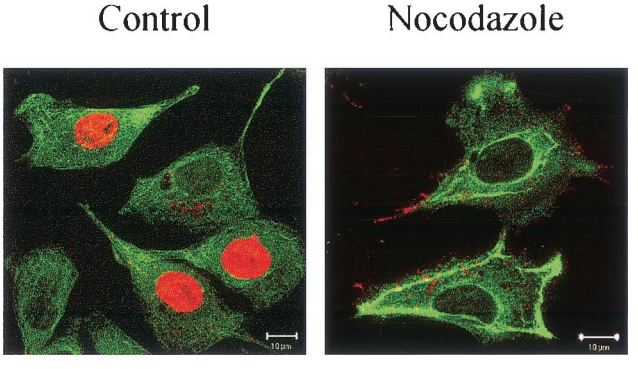

FIG. 5. Effect of nocodazole on intracellular distribution of tubulin and on localization of CPV. The analysis was carried out by immunofluorescence microscopy at 12 h p.i. Control, without nocodazole; nocodazole, nocodazole at 60 μM. Color: red, CPV; green, microtubules. Bar, 10 μm.

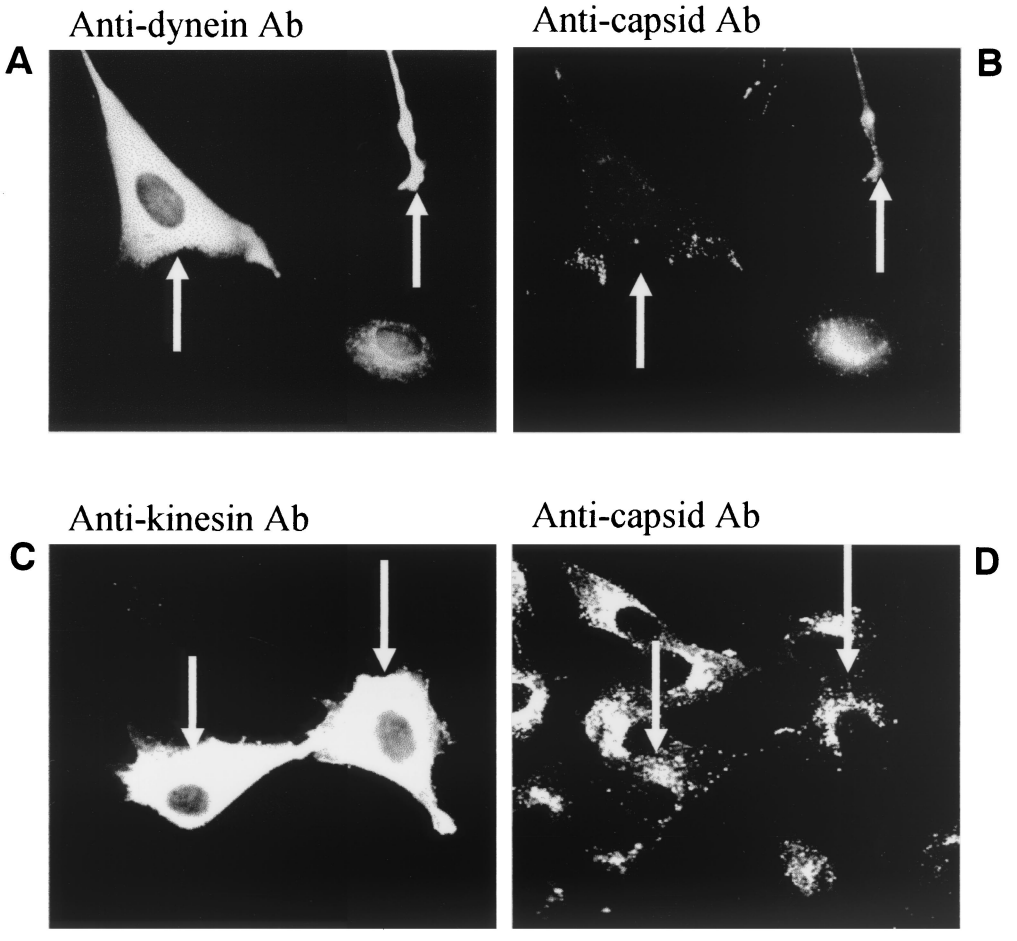

FIG. 6. Effect of microinjected anti-dynein and anti-kinesin antibody on CPV entry. The antibodies were microinjected into the cytoplasm of NLFK cells, after which the cells were inoculated with CPV. Cells were fixed at 2 h p.i. Microinjected cells are indicated by arrows. Noninjected cells serve as controls. (A) Injected antibody to dynein visualized with fluorescein isothiocyanate-conjugated anti-mouse antibody. (B) Cells injected with anti-dynein antibody, CPV detected with polyclonal anti-capsid antibody and TRITC-conjugated anti-rabbit antibody. (C) Cells microinjected with anti-kinesin antibody indicated by arrows. Injected antibody was detected as in panel B. (D) Cells injected with anti-kinesin antibody indicated by arrows. CPV was detected as described above.

with CPV. In immunoelectron microscopy analysis of cells fixed at at 1 h p.i., gold particles were found in endosomes having a complex, onion-like structure with internal membranes (Fig. 7A). These endosomes had morphology resembling that of late endosomes. At 3 h p.i., gold particles were in vesicles with complex internal membranes and a heterogeneous interior (Fig. 7B), resembling lysosomes. To detect whether gold labeling had changed the route of virus particles in preembedding studies, cryosections made from infected cells were fixed and subsequently immunolabeled. In these experiments CPV was found at 1 h or at 3 h p.i. in similar vesicular structures as in preembedded samples, even though the intracellular fine structure had suffered from cryosectioning (Fig. 7C and D). We thus conclude that gold label did not affect the intracellular route of CPV and that the results obtained with preembedding electron microscopy suggest a genuine lysosomal location of CPV.

These findings were supported by double-labeling immunofluorescence experiments. The staining patterns of the following markers for the trans-Golgi and endosomal vesicles were compared with that of CPV during the time periods p.i. indicated in parentheses: endocytosed transferrin (0 to 8 h), TGN-38 (0 to 8 h), β-COP (0 to 3 h), MPR (0 to 3 h), PDI (0 to 8 h), and LAMP-2 (0 to 8 h). For control, the staining patterns of these markers in infected cells and in mock-infected control cells were compared. CPV infection did not change the subcellular distribution of the organelles stained with these antibodies (results not shown).

We found a strong colocalization of CPV with endocytosed transferrin, a marker of recycling endosomes (Fig. 8). This colocalization was essentially complete from 0.5 to 1 h p.i., when both transferrin and CPV appeared to move from the cellular periphery to the perinuclear area (cf. data at 0.5 h p.i. with those at 1 and 3 h p.i. in Fig. 8), and it was evident, although less extensive, even at 8 h p.i. (Fig. 8). MPR, a marker of late endosomes, colocalized significantly with CPV at 0.5 h p.i. and extensively at 1 h p.i., with some weak colocalization being observable even at 3 h p.i. (Fig. 8). A change with time in the location of CPV from a pericellular location toward a perinuclear location with an increasing overlap with the MPR-containing area is evident from these data (Fig. 8).

The lysosomal protein LAMP-2, which was found in perinu-

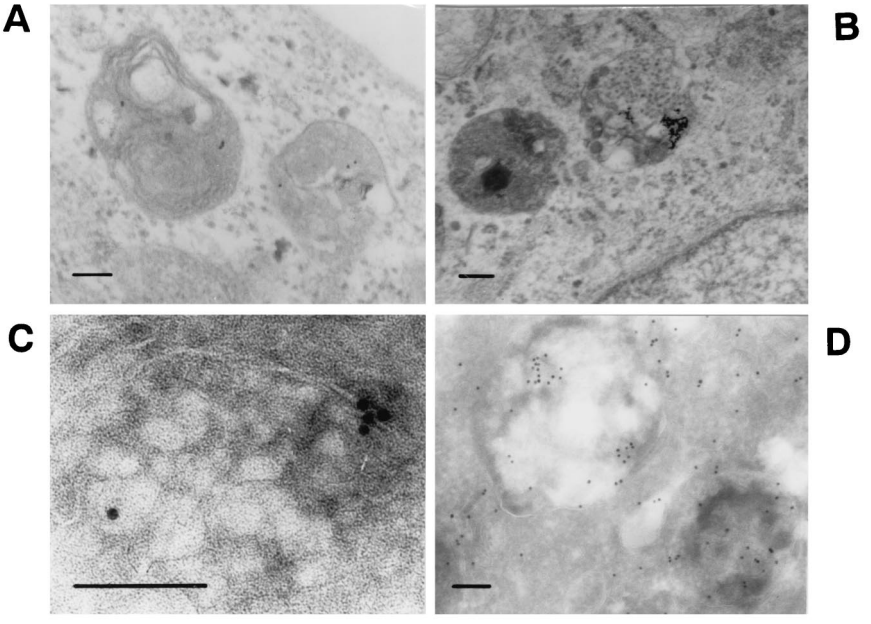

FIG. 7. Immunoelectron microscopy analysis of CPV-containing vesicles. For technical details, see the legend to Fig. 1. Bars, 100 nm. (A) Preembedding at 1 h p.i.; (B) preembedding at 3 h p.i.; (C) cryosection at 1 h p.i.; (D) cryosection at 3 h p.i.

clear vesicles, showed weak colocalization with CPV at 30 min p.i. but a strong colocalization at 1 h p.i. and later during the 8 h it was monitored (Fig. 8). The immunofluorescence images suggested that the colocalization was at its most intense at 3 h p.i. In contrast, there was no colocalization of CPV with TGN-38 (Fig. 9). This marker was found in a crescent perinuclear vesicular compartment and also in small peripherally located structures. The perinuclear vesicles showing the presence of PDI and CPV had a distinct, nonoverlapping staining pattern up to 8 h p.i. (Fig. 9). Antibody to β-COP, which binds to the β-subunit containing coatomer proteins generally found in Golgi subcompartments, revealed a distinct staining pattern which did not overlap with that of CPV (not shown). Taken together, these results suggest that, after it enters cells in coated vesicles, CPV is trafficked to the recycling compartment and then to the late endosomes, followed by the lysosomes. However, caution is advised here since we also found some colocalization of transferrin with LAMP-2 (not shown). Thus, this marker may not be absolutely specific to recycling endosomes.

An important challenge of the present experimental setup is to show that it is the route of infective particles that is being followed. To ensure this, empty (L-CPV) and full (H-CPV) capsids were prepared, and their entry routes were followed separately. Both empty and full capsids were found to be trafficked identically into the lysosomal compartment (Fig. 10). Thus, the data show that empty and full particles undergo a similar endocytic trafficking and reach the late endosomal and lysosomal compartments. Therefore, the endocytic route revealed in the above experiments must be the route used by infective particles. In support of this, viral DNA visualized by fluorescence in situ hybridization and viral capsid proteins were observed in perinuclear vesicular structures from 8 to 10 h after viral uptake (Fig. 11). At 9 to 12 h p.i., viral DNA was detected in the nucleus (Fig. 11).

DISCUSSION

The intracellular entry pathways of nonenveloped viruses are still not well understood (18). Here we have characterized in detail the intracellular entry route of CPV in NLFK cells by monitoring the intracellular pathways of CPV capsid proteins and CPV DNA during entry.

After it bound to the cell surface, CPV was internalized in endocytic vesicles within minutes (Fig. 1 and 2). From 30 min to 10 h p.i., CPV was found in perinuclear vesicles (Fig. 1). From control experiments we know that viral proliferation, detected as the presence of NS1 protein of CPV in the nucleus, was active at 8 h p.i. Thus, the time frame of the entry phase extends a few hours from inoculation. During that time CPV must find its way to the correct endosomal compartment(s) where penetration of its genome into the cytoplasm can take place.

CPV was initially detected at the plasma membrane by using electron microscopy (Fig. 2A). Clusters containing a number of gold particles were observed in pits, which had an electron-dense coating resembling clathrin. In samples fixed at 5 min p.i., CPV was found both in clathrin-coated vesicles (Fig. 2B) and in noncoated, endosome-like vesicles (Fig. 2C). This was expected, since the clathrin coat is known to disassemble from vesicles within 1 to 3 min after pinching off from the plasma membrane (22). To study whether the clathrin-dependent route was the exclusive route used by CPV, we used immunoelectron microscopy to determine whether CPV could also be detected also in other kind of vesicles immediately after intake (Fig. 3A). We also carried out double-labeling immunofluorescence analysis to search for possible colocalization of CPV with caveolae (Fig. 3B). Both analyses failed to show any association of CPV with caveolae or caveolin (Fig. 3A and B). Our results thus support the idea that CPV enters the host cells by clathrin-mediated endocytosis (26).

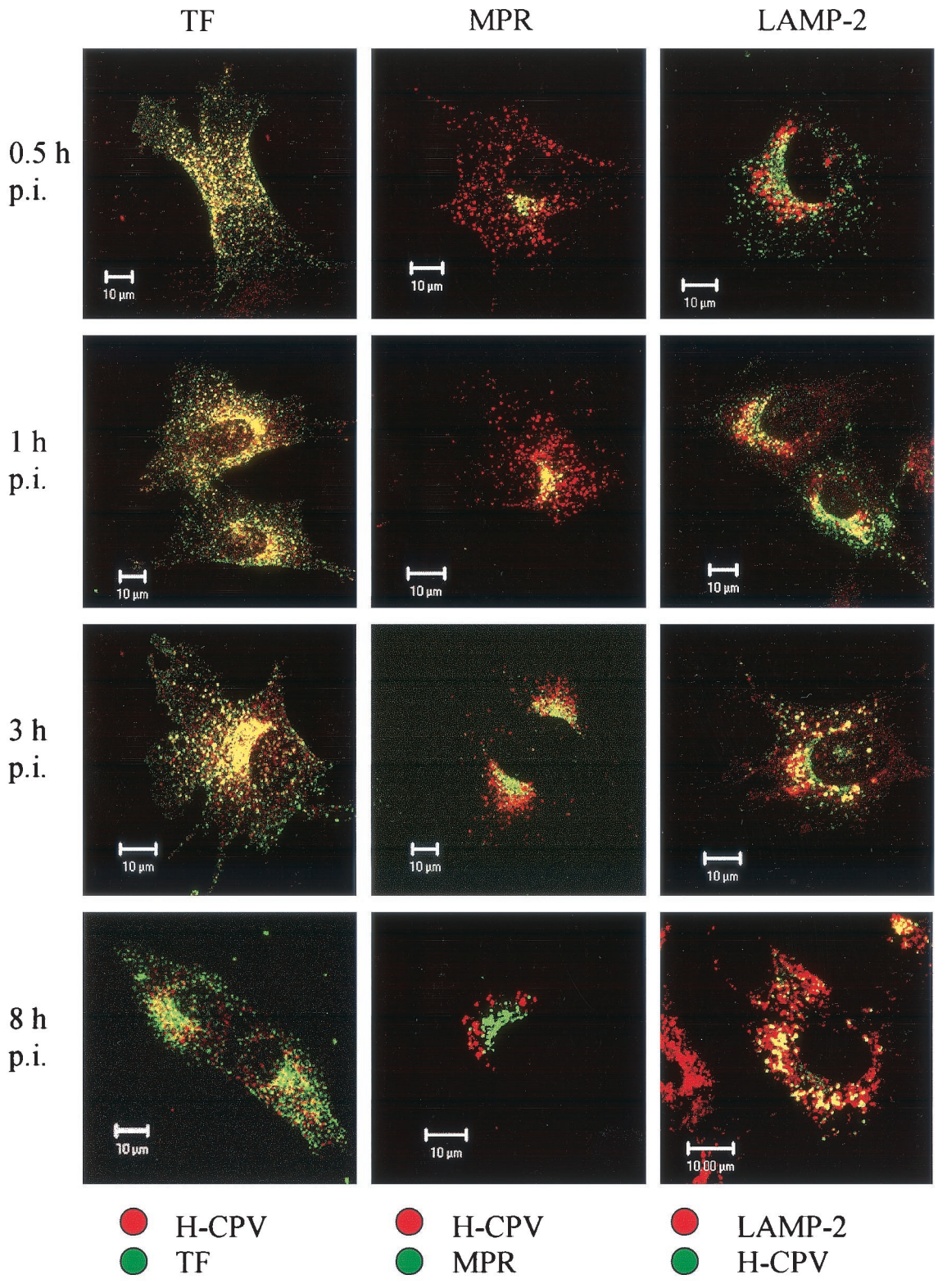

FIG. 8. Colocalization of full CPV capsids (H-CPV) and the organelle markers TF, MPR, and LAMP-2. The infected cells were fixed at various time points p.i. as indicated on the left. Left column: TF, green; L-CPV, red. Middle column: MPR, green; L-CPV, red. Right column: L-CPV, green; LAMP-2, red. In all columns, colocalization is yellow. Bars, 10 μm.

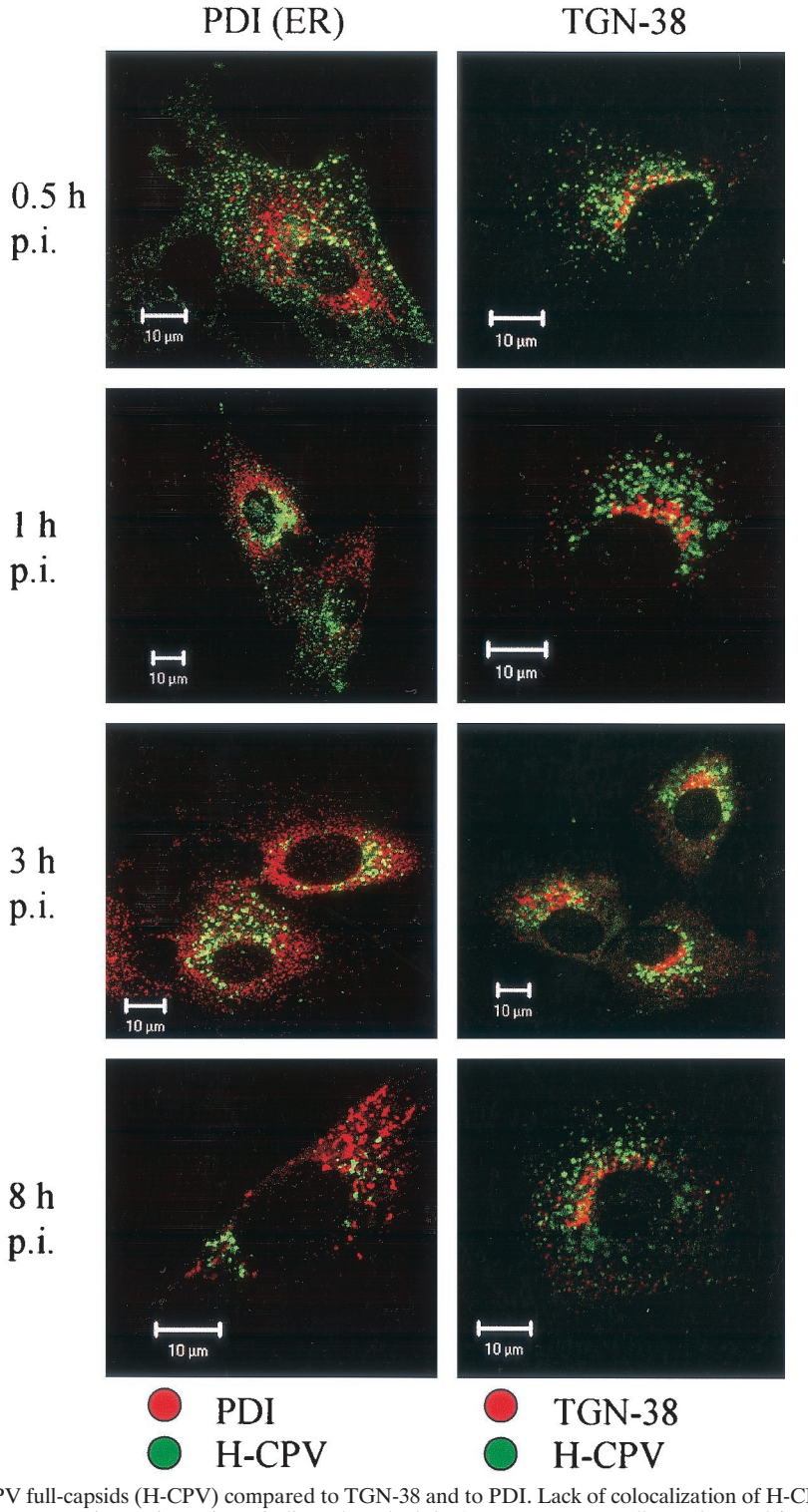

FIG. 9. Localization of CPV full-capsids (H-CPV) compared to TGN-38 and to PDI. Lack of colocalization of H-CPV with trans-Golgi marker TGN-38 and/or with ER marker PDI. Time points p.i. are indicated on the left. CPV, green; organelle marker, red (TGN-38, PDI); colocalization, yellow.

According to earlier studies, CPV infection can be blocked by raising the endosomal pH (3, 26, 44) or by the microtubule-disrupting drug nocodazole (44). Furthermore, low temperature inhibits the infection, suggesting the involvement of microtubule-dependent vesicle traffic (44). In the present study CPV was detected in microtubule-associated vesicles (Fig. 4). Furthermore, disruption of the microtubule network with nocodazole inhibited infection and caused vesicles containing CPV to dissociate from the microtubules and disperse to the periphery of the cells (Fig. 5). In the immunoelectron micro-

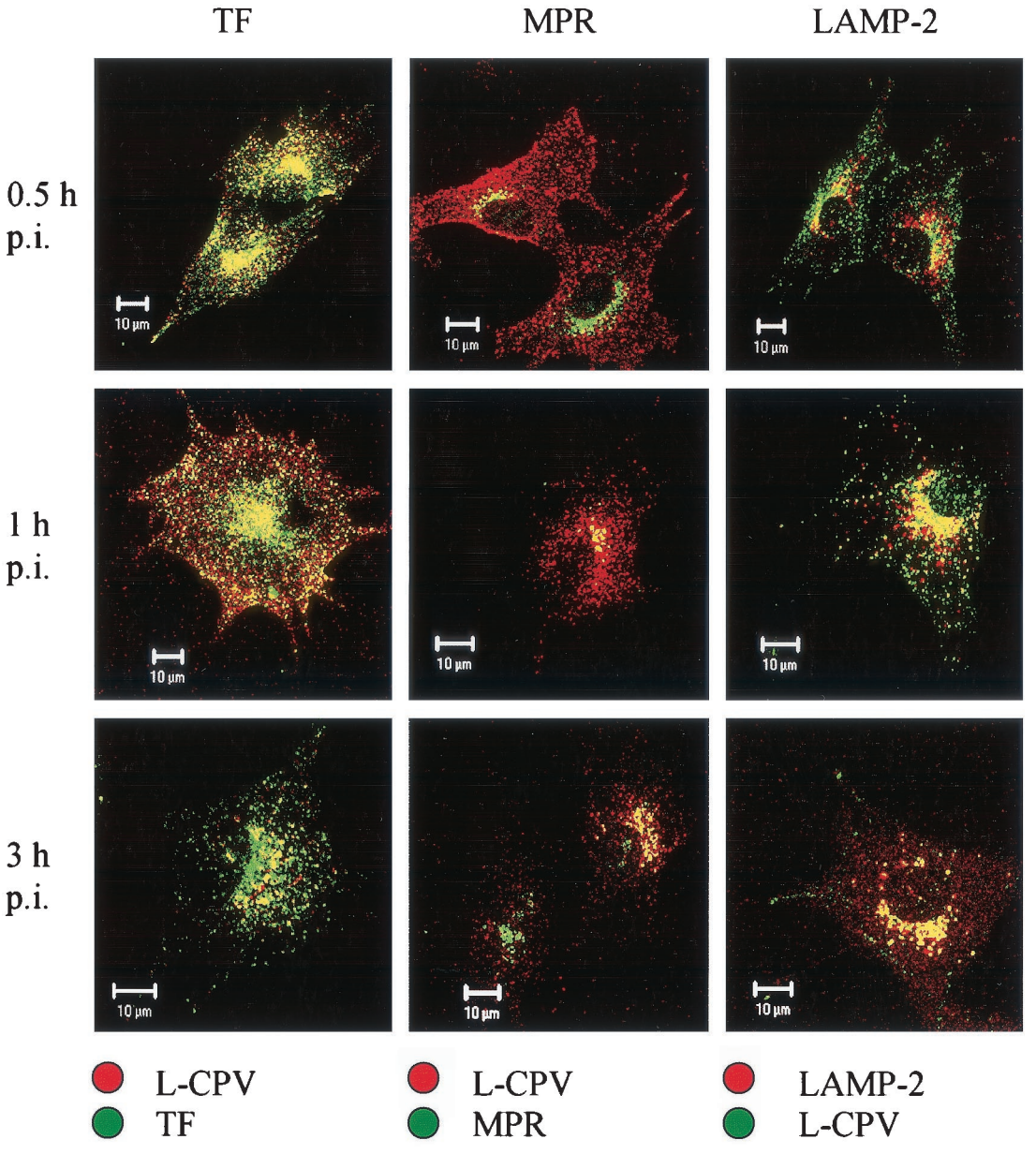

FIG. 10. Colocalization of empty CPV capsids (L-CPV) and the organelle markers TF, MPR, and LAMP-2. The infected cells were fixed at time points p.i. indicated on the left. Left column: TF, green, L-CPV red. Middle column: MPR, green, L-CPV, red. Right column: L-CPV, green, LAMP-2, red. In all columns, the colocalization is yellow. Bars, 10 μm.

graphs (Fig. 4), electron-dense material was seen connecting the vesicle to the microtubule. This led us to test the effects on entry of cytoplasmically microinjected anti-dynein and anti-kinesin antibodies. Microinjected anti-dynein antibody caused endocytosed CPV to distribute in peripherally oriented vesicles, which was quite different from the orientation seen in infected, noninjected cells (see Fig. 1). The effect caused by microinjected anti-dynein antibody appeared quite similar to that caused by nocodazole (Fig. 5 and 6). In contrast, cytoplasmically injected anti-kinesin antibody did not affect the intracellular transport of CPV (Fig. 6). Thus, the findings of the present and previous studies support the view that vesicular transport of CPV to perinuclear area takes place along microtubules and is dependent on dynein. This conclusion fits well with the idea that the endocytic trafficking from the early endosome to the late or to the recycling endosome is dependent on microtubules (14, 30, 31) and that the dynein or dynactin motor plays a critical role in the translocation of endosomal vesicles along microtubules (43). Dynamin, which facilitates the budding of clathrin-coated pits, has been shown to be essential for the entry of AAV (1) and CPV (26).

Many microorganisms, such as *Listeria monocytogenes*, *Shigella flexneri*, *Rickettsia* spp., vaccinia virus, and most likely also baculovirus, are known to use cellular actin to travel through an infected host cell (reviewed in reference 34). The disruption of actin cytoskeleton with cytochalasin D did not cause any

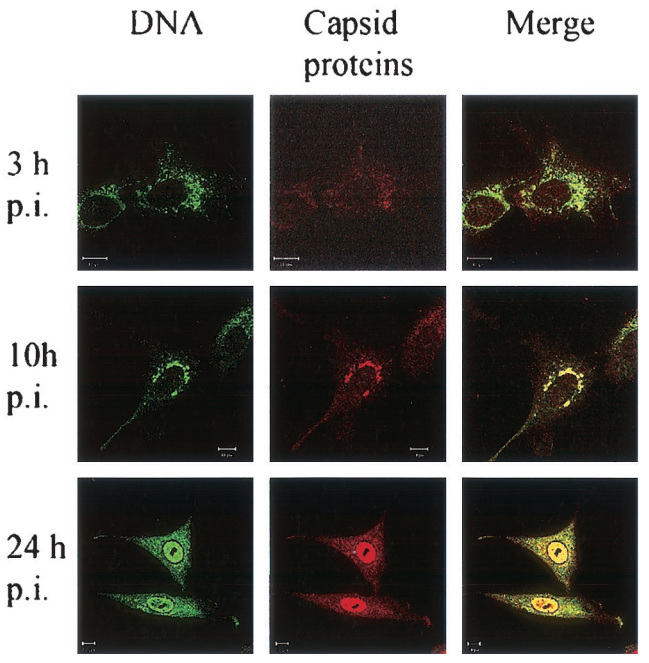

FIG. 11. Localization of CPV-DNA and capsid proteins during infection. Viral DNA was detected by fluorescence in situ hybridization, and polyclonal antibody was used to stain capsid proteins. The time points p.i. are indicated on the left.

significant effect on the entry of CPV (our unpublished data), which suggests that actin is not needed for CPV entry.

An important aim of our study was to define the vesicular compartments that are utilized by CPV in its entry. It was earlier shown that CPV particles colocalize with transferrin in Mv1Lu cells transfected with the transferrin receptor (26). In the present study, we found CPV to colocalize with transferrin in NLFK cells at 0 to 3 h p.i. and to a lesser degree at 8 h p.i. (Fig. 8). From 0.5 to 3 h p.i., both transferrin and CPV moved from peripherally located vesicles to perinuclear vesicles (Fig. 8). Since transferrin is a well-known representative of endocytosed molecules traveling through the recycling endosomes (20), the data strongly suggest that CPV reached this compartment at one stage during its entry. From the recycling endosomes, a degradative route diverts via late endosomes to lysosomes (20). The immunoelectron microscopy data (Fig. 7) and the observed colocalization (Fig. 8) of CPV with MPR, a marker of late endosomes, suggest that CPV was transported from recycling endosomes to late endosomes.

At 3 h p.i., CPV was observed exclusively in vesicles with a polar perinuclear location. We define these vesicles as lysosomes for the following reasons. First, even though the location of these vesicles resembled that of the Golgi apparatus, they did not colocalize with the Golgi marker, TGN-38 (22) (Fig. 9). Second, no colocalization was found between the ER marker (PDI) and CPV-containing vesicles at 0.5 to 8 h p.i. (Fig. 9). Third, as determined by immunoelectron microscopy at 3 h p.i., the vesicles had internal membranes and a polymorphous interior (Fig. 7B) that were different from the onion-like vesicles observed earlier (Fig. 7A). The characteristics of the vesicles in Fig. 7B agree with the description given of lysosomes (24). Control experiments with cryosectioning showed that labeling CPV with antibody and colloidal gold did not change its entry route (Fig. 7C and D). Finally, LSM imaging showed that, at 1 to 8 h p.i. CPV was in extensive colocalization with the major lysosomal membrane protein LAMP-2 (Fig. 8). It is also significant that CPV DNA was found in perinuclear vesicles at 10 h p.i. (Fig. 11). Taken together, these results suggest that CPV enters the lysosomes before it is released from the vesicular compartment.

Empty CPV capsids (without DNA, L-CPV) seemed to use the same intracellular route as full capsids during the first 3 h of infection (Fig. 10). They were internalized with transferrin and entered the recycling route. At 1 h after uptake, the L-CPV particles were detected in late endosomes and at 3 h in lysosomal vesicles. This finding indicates that, at least to the point of release from the endosomal compartment, the DNA of CPV does not have a role in the vesicular transport of the virion. The routing of virus particles from the recycling pathway to the degradative route might be necessary for release of the virus from the vesicles. It is known that polyvalent ligands are able to cross-link proteins which normally recycle. Coupling of these receptors changes their route to the degradative pathway. This misrouting has been demonstrated with transferrin made polyvalent by coupling to colloidal gold, with anti-receptor antibody, and with multivalent transferrin (11, 15, 20, 37). It is possible that CPV cross-links transferrin receptors and changes their route to the degradative pathway.

It has been shown earlier that the microinjection of capsid antibodies into the cytoplasm of a CPV-infected cell could prevent proliferation of CPV, even when carried out as late as 6 h p.i. (44). These findings suggest that CPV is released from the vesicles several hours after uptake and that viral DNA is released with capsid proteins attached to it. In the present study, CPV DNA or CPV capsid proteins were not detected in the cytoplasm before replication. These observations may indicate that the release of CPV into the cytoplasm is very slow or occurs at very low levels. Thus, the behavior of CPV is in considerable contrast to that of AAV (2), which is able to penetrate the endosomal membrane quickly after internalization. Due to the fact that the CPV capsid proteins were still detected in LAMP-2-positive vesicles 8 h after uptake and CPV capsid proteins were detected in close contact with DNA, it is presumable (although not proven) that the lysosomal compartment is the site of viral release from the vesicles. Similarly, adenovirus serotype 7 has been shown to colocalize with the lysosomal marker protein (α_2-macroglobulin). Porcine parvovirus has shown to colocalize with LAMP-2 before escape from vesicular structures (23, 46).

Our results suggest that CPV entry involves at least five different steps: (i) binding and clustering to the coated pits on the cell surface, followed by uptake in the coated vesicles; (ii) entry to the early endosomes; (iii) transport from the peripheral area to the perinuclear region in recycling endosomes along microtubules in a dynein-dependent manner; (iv) viral entry into the LAMP-2-positive vesicles via late endosomes; and (v) release of viral material from vesicles prior to transport to the nucleus. The mechanisms of CPV uncoating and escape from vesicles have not yet been fully characterized.

ACKNOWLEDGMENTS

We thank Klaus Hedman (University of Helsinki, Helsinki, Finland) for critically reading the manuscript. We also thank Pirjo Kauppinen and Raija Vassinen for skillful technical assistance.

This work was supported by the National Technology Agency (TEKES).

REFERENCES

1. **Anderson, H. A., Y. Chen, and L. C. Norkin.** 1996. Bound simian virus 40 translocates to caveolin-enriched membrane domains, and its entry is inhibited by drugs that selectively disrupt caveolae. Mol. Biol. Cell **7:**1825–1834.
2. **Bartlett, J. S., R. Wilcher, and R. J. Samulski.** 2000. Infectious entry pathway of adeno-associated virus and adeno-associated virus vectors. J. Virol. **74:** 2777–2785.
3. **Basak, S., and H. Turner.** 1992. Infectious entry pathway for canine parvovirus. Virology **186:**368–376.
4. **Bayer, N., D. Schober, E. Prachla, R. F. Murphy, D. Blaas, and R. Fuchs.** 1998. Effect of bafilomycin A1 and nocodazole on endocytic transport in HeLa cells: implications for viral uncoating and infection. J. Virol. **72:**9645–9655.
5. **Blumenthal, R., P. Seth, M. C. Willingham, and I. Pastan.** 1986. pH-dependent lysis of liposomes by adenovirus. Biochemistry **25:**2231–2237.
6. **Curry, S., M. Chow, and J. M. Hogle.** 1996. The poliovirus 135S particle is infectious. J. Virol. **70:**7125–7131.
7. **Douar, A. M., K. Poulard, D. Stockholm, and O. Danos.** 2001. Intracellular trafficking of adeno-associated virus vectors: routing to the late endosomal compartment and proteasome degradation. J. Virol. **75:**1824–1833.
8. **Dryen, K. A., G. Wang, M. Yeager, M. L. Nibert, K. M. Coombs, D. B. Furlong, B. N. Fields, and T. S. Baker.** 1993. Early steps in reovirus infection are associated with dramatic changes in supramolecular structure and protein conformation: analysis of virions and subviral particles by cryoelectron microscopy and image reconstruction. J. Cell Biol. **122:**1023–1041.
9. **Duan, D., Q. Li, A. W. Kao, Y. Yue, J. E. Pessin, and J. F. Engelhardt.** 1999. Dynamin is required for recombinant adeno-associated virus type 2 infection. J. Virol. **73:**10371–10376.
10. **Fenner, F., P. A. Bachmann, E. P. J. Gibbs, F. A. Murphy, M. J. Studdert, and D. O. White.** 1987. Veterinary virology. Academic Press, Inc., Orlando, Fla.
11. **Fodor, I., A. Egyed, and G. Lelkes.** 1986. A comparative study on the cellular processing of free and gold-conjugated transferrin. Eur. J. Cell Biol. **42:**74–78.
12. **Fricks, C. E., and J. M. Hogle.** 1990. Cell-induced conformational change in poliovirus: externalization of the amino terminus of VP1 is responsible for liposome binding. J. Virol. **64:**1934–1945.
13. **Greber, U. F., M. Willetts, P. Webster, and A. Helenius.** 1993. Stepwise dismantling of adenovirus 2 during entry into cells. Cell **75:**477–486.
14. **Gruenberg, J., G. Griffiths, and K. E. Howell.** 1989. Characterization of the early endosome and putative endocytic carrier vesicles in vivo and with assay of vesicle fusion in vitro. J. Cell Biol. **108:**1301–1316.
15. **Gruenberg, J., and K. E. Howell.** 1989. Membrane traffic in endocytosis: insights from cell-free assays. Annu. Rev. Cell Biol. **5:**453–481.
16. **Huovila, A. P., A. M. Eder, and S. D. Fuller.** 1992. Hepatitis B surface antigen assembles in a post-ER, pre-Golgi compartment. J. Cell Biol. **118:** 1305–1320.
17. **Kaludov, N., K. E. Brown, R. W. Walters, J. Zabner, and J. A. Chiorini.** 2001. Adeno-associated virus serotype 4 (AAV4) and AAV5 both require sialic acid binding for hemagglutination and efficient transduction but differ in sialic acid linkage specificity. J. Virol. **75:**6884–6893.
18. **Kasamatsu, H., and A. Nakanishi.** 1998. How do animal DNA viruses get to the nucleus? Annu. Rev. Microbiol. **52:**627–686.
19. **Marjomaki, V. S., A. P. Huovila, M. A. Surkka, I. Jokinen, and A. Salminen.** 1990. Lysosomal trafficking in rat cardiac myocytes. J. Histochem. Cytochem. **38:**1155–1164.
20. **Marsh, E. W., P. L. Leopold, N. L. Jones, and F. R. Maxfield.** 1995. Oligomerized transferrin receptors are selectively retained by a lumenal sorting signal in a long-lived endocytic recycling compartment. J. Cell Biol. **129:** 1509–1522.
21. **Martinez, C. G., R. Guinea, J. Benavente, and L. Carrasco.** 1996. The entry of reovirus into L cells is dependent on vacuolar proton-ATPase activity. J. Virol. **70:**576–579.
22. **Mellman, I.** 1996. Endocytosis and molecular sorting. Annu. Rev. Cell Dev. Biol. **12:**575–625.
23. **Miyazawa, N., R. G. Crystal, and P. L. Leopold.** 2001. Adenovirus serotype 7 retention in a late endosomal compartment prior to cytosol escape is modulated by fiber protein. J. Virol. **75:**1387–1400.
24. **Mukherjee, S., R. N. Ghost, and R. Maxfield.** 1997. Endocytosis. Physiol. Rev. **77:**759–803.
25. **Parker, J. S., W. J. Murphy, D. Wang, S. J. O'Brien, and C. R. Parrish.** 2001. Canine and feline parvoviruses can use human or feline transferrin receptors to bind, enter, and infect cells. J. Virol. **75:**3896–3902.
26. **Parker, J. S., and C. R. Parrish.** 2000. Cellular uptake and infection by canine parvovirus involves rapid dynamin-regulated clathrin-mediated endocytosis, followed by slower intracellular trafficking. J. Virol. **74:**1919–1930.
27. **Parker, J. S. L., and C. R. Parrish.** 1997. Canine parvovirus host range is determined by the specific conformation of additional region of the capsid. J. Virol. **71:**9214–9222.
28. **Pelkmans, L., J. Kartenbeck, and A. Helenius.** 2001. Caveolar endocytosis of simian virus 40 reveals a new two-step vesicular-transport pathway to the ER. Nat. Cell Biol. **3:**473–483.
29. **Pérez, L., and L. Carrasco.** 1993. Entry of poliovirus into cells does not require a low-pH step. J. Virol. **67:**4543–4548.
30. **Ren, M., G. Xu, J. Zeng, C. De Lemos-Chiarandini, M. Adesnik, and D. D. Sabatini.** 1998. Hydrolysis of GTP on rab11 is required for the direct delivery of transferrin from the pericentriolar recycling compartment to the cell surface but not from sorting endosomes. Proc. Natl. Acad. Sci. USA **95:** 6187–6192.
31. **Sakai, T., S. Yamashina, and S. Ohnishi.** 1991. Microtubule-disrupting drugs blocked delivery of endocytosed transferrin to the cytocenter, but did not affect return of transferrin to plasma membrane. J. Biochem. **109:**528–533.
32. **Seth, P.** 1994. Mechanism of adenovirus-mediated endosome lysis: role of the intact adenovirus capsid structure. Biochem. Biophys. Res. Commun. **205:**1318–1324.
33. **Stang, E., J. Kartenbeck, and R. G. Parton.** 1997. Major histocompatibility complex class I molecules mediate association of SV40 with caveolae. Mol. Biol. Cell **8:**47–57.
34. **Stidwill, R. P., and U. F. Greber.** 2000. Intracellular virus trafficking reveals physiological characteristics of the cytoskeleton. News Physiol. Sci. **15:**67–71.
35. **Strassheim, M. L., A. Gruenberg, P. Veijalainen, J.-Y. Sgro, and C. R. Parrish.** 1994. Two dominant neutralizing antigenic determinants of canine parvovirus are found on the threefold spike of the virus capsid. Virology **198:**175–184.
36. **Summerford, C., and R. J. Samulski.** 1998. Membrane-associated heparan sulfate proteoglycan is a receptor for adeno-associated virus type 2 virions. J. Virol. **72:**1438–1445.
37. **Takizava, T., and J. M. Robinson.** 1994. Use of 1.4-nm immunogold particles for immunocytochemistry on ultra-thin cryosections. J. Histochem. Cytochem. **42:**1615–1623.
38. **Tattersall, P., and S. F. Cotmore.** 1988. The nature of parvoviruses, p. 5–41. *In* J. R. Pattison (ed.), Parvoviruses and human disease. CRC Press, Boca Raton, Fla.
39. **Tokuyasu, K. T.** 1978. A study of positive staining of ultrathin frozen sections. J. Ultrastruct. Res. **63:**287–307.
40. **Tokuyasu, K. T.** 1973. A technique for ultracryotomy of cell suspensions and tissues. J. Cell Biol. **57:**551–565.
41. **Tosteson, M. T., and M. Chow.** 1997. Characterization of the ion channels formed by poliovirus in planar lipid membranes. J. Virol. **71:**507–511.
42. **Tosteson, M. T., M. L. Nibert, and B. N. Fields.** 1993. Ion channels induced in lipid bilayers by subvirion particles of the nonenveloped mammalian reoviruses. Proc. Natl. Acad. Sci. USA **90:**10549–10552.
43. **Valetti, C., D. M. Wetzel, M. Schrader, M. J. Hasbani, S. R. Gill, T. E. Kreis, and T. A. Schroer.** 1999. Role of dynactin in endocytic traffic: effects of dynamitin overexpression and colocalization with CLIP-170. Mol. Biol. Cell **10:**4107–4120.
44. **Vihinen-Ranta, M., A. Kalela, P. Mäkinen, L. Kakkola, V. Marjomäki, and M. Vuento.** 1998. Intracellular route of canine parvovirus entry. J. Virol. **72:** 802–806.
45. **Vihinen-Ranta, M., W. Yuan, and C. R. Parrish.** 2000. Cytoplasmic trafficking of the canine parvovirus capsid and its role in infection and nuclear transport. J. Virol. **74:**4853–4859.
46. **Zádori, Z., J. Szelei, M.-C. Lacoste, Y. Li, S. Gariépy, P. Raymond, M. Allaire, I. R. Nabi, and P. Tijssen.** 2001. A viral phospholipase A_2 is required for parvovirus infectivity. Dev. Cell **1:**291–302.